Chinese Journal of Mechanical Engineering

ORIGINAL ARTICLE

Open Access

Novel Batch Polishing Method of Ceramic Cutting Inserts for Reducing Tool Wear

Rui Gao[1], Chunjin Wang[1*], Yee Man Loh[1], Xiaoliang Liang[1], Chen Jiang[2] and Chi Fai Cheung[1*]

Abstract

Ceramic cutting inserts are a type of cutting tool commonly used in high-speed metal cutting applications. However, the wear of these inserts caused by friction between the workpiece and cutting inserts limits their overall effectiveness. In order to improve the tool life and reduce wear, this study introduces an emerging method called magnetic field-assisted batch polishing (MABP) for simultaneously polishing multiple ceramic cutting inserts. Several polishing experiments were conducted under different conditions, and the wear characteristics were clarified by cutting S136H steel. The results showed that after 15 min of polishing, the surface roughness at the flank face, edge, and nose of the inserts was reduced to below 2.5 nm, 6.25 nm, and 45.8 nm, respectively. Furthermore, the nose radii of the inserts did not change significantly, and there were no significant changes in the weight percentage of elements before and after polishing. Additionally, the tool life of the batch polished inserts was found to be up to 1.75 times longer than that of unpolished inserts. These findings suggest that the MABP method is an effective way to mass polish ceramic cutting inserts, resulting in significantly reduced tool wear. Furthermore, this novel method offers new possibilities for polishing other tools.

Keywords Polishing, Finishing, Magnetic field-assisted, Tool wear, Ultra-precision machining

1 Introduction

Nowadays, a machining tool is essential for shaping processes in a wide range of industrial applications [1]. Since it contacts with the workpiece and influences the machining quality and efficiency of the workpiece directly, the cutting insert plays a vital role in the machining tool [2, 3]. In recent years, various cutting insert materials, including cemented carbide [4], cermet [5], ceramic [6], polycrystalline diamond (PCD) [7], and cubic-boron-nitride (CBN) [8], have been developed and successfully implemented concerning different machining conditions. Among them, ceramic cutting inserts have been widely applied for the finishing of cast iron and hardened materials due to their mechanical properties and chemical stability at high temperatures [9, 10]. However, recent pieces of evidence suggest that some undesirable characteristics, such as the friction at the insert-chip interface [11, 12] and machining marks on the insert surface [13], can accelerate the wear of ceramic cutting inserts. As a result, an effective and efficient approach to achieve a notable extension of the tool life during machining is urgently needed.

Up to present, several studies have reported that cryogenic coolant [14], coating [15], changing insert shapes [16], and process parameters [17] are employed for improving the cutting insert life. The cryogenic coolant is carried out at lower the machining temperature to improve insert life [18]. However, conventional cutting oil is considered harmful to the environment [19] and shows low cooling efficiency [20]. Moreover, cryogenic

*Correspondence:
Chunjin Wang
chunjin.wang@polyu.edu.hk
Chi Fai Cheung
benny.cheung@polyu.edu.hk
[1] State Key Laboratory of Ultra-precision Machining Technology, Department of Industrial and Systems Engineering, The Hong Kong Polytechnic University, Hong Kong 999077, China
[2] College of Mechanical Engineering, University of Shanghai for Science and Technology, Shanghai 200093, China

coolants using liquid nitrogen are not suitable for long-term processing because they are normally used in industrial applications [21]. In the coating process, chemical vapor deposition (CVD) [22] and physical vapor deposition (PVD) [23] methods are now frequently applied for cutting inserts corresponding to different applications. Due to the extremely high requirement on the cutting insert surface quality, the coating materials and equipment are relatively expensive [24]. Although the technique to alter insert shapes and process parameters is constantly advancing, there are still several steps for preparing a micro-texture cutting insert [25]. In addition, the grinding marks and micro-defects on the insert surface remain unresolved [26].

Compared with the aforementioned technologies, some researchers have proven that polishing does not require expensive machine equipment and can smooth the insert surface, reduce the friction on the insert-chip interface and eliminate machining marks simultaneously [27, 28]. In 1997, Yoshikawa et al. [29] reported a hot-iron-metal method (HIMM) as the polishing method for the coated cutting insert. They also developed an apparatus to polish cutting insert flank by HIMM. To polish inserts flank with complex shapes, Lyu et al. [30] found that the shear thickening polishing (STP) method achieves precision polishing of cutting insert, and the optimal combination of parameters was obtained as well. In a follow-up study, brush tool-assisted shear thickening polishing (B-STP) was proposed to break the thickened agglomerates and improve the slurry flow ability, and the surface roughness of cutting insert flank could reach 7.9 nm after 15 min of polishing [13]. Yamaguchi et al. [31] proposed a polishing method, named magnetic abrasive finishing (MAF), to smooth cutting insert nose and flank, and the treated insert life was extended by 150%. On the other hand, the edges of the as-received cutting inserts are uneven [32], which increases friction and accelerates cutting insert wear. Tanaka et al. [33] provided a polishing approach of cutting insert edge using an AC electric field which was applied between the polishing pad and the cutting insert. A smooth edge of the inserts was obtained, and the tool life of polished inserts tended to be longer than unpolished ones. But the whole process consisted of four steps because of the equipment limitations. Ishimarua et al. [34] and Izumi et al. [35] studied the polishing performance of the cutting insert edge by ultraviolet-ray irradiation-assisted polishing. After treatment, the radii of the insert edge decreased slightly. However, the surface roughness of the cutting inserts is very dependent on the quartz glass polishing plate [32]. For improving the polishing efficiency of individual cutting inserts, the plasma electrolytic polishing (PEP) method was employed by An et al. [1]. A better-polished surface of the coated cutting insert was obtained with the voltage of 110 V, but the surface roughness (Ra) only stayed at a deep sub-micron level with 0.096 μm [36]. Although some research has been carried out on polishing cutting inserts, no single study exists which provides a batch polishing machine for smoothing flank, nose, and edge simultaneously with nanometer scale surface roughness. Meanwhile, other mainstream polishing methods such as bonnet polishing [37, 38], fluid jet polishing [39, 40] and magnetorheological finishing [41, 42] are not suitable for the polishing of cutting inserts due to the high equipment cost and polishing cost.

This paper presents a novel method, called 'magnetic field-assisted batch polishing (MABP)', for automatic batch polishing cutting inserts simultaneously, together with nanometer scale surface finish. Section two of this paper will examine the working principle of the MABP method. Hence, a series of polishing and turning experiments are carried out. The fourth section presents the findings of the research, focusing on the four key themes including polishing performance, surface roughness, element composition, and nose radius. Meanwhile, the possibility of batch polishing by MABP will be examined through multiple insert polishing in Section 4 as well. Section 5 analyses the effects of MABP processing on cutting insert life by cutting S136H steel.

2 Materials and Methods

2.1 Sample Preparation

Ceramics inserts are capable of running at high speeds, thus reducing expensive machining time [43]. In addition, ceramic maintains good surface finishes due to its low affinity to workpiece materials [44]. Accordingly, one commercially available uncoated triangular ceramic cutting inserts (TNGA160404), manufactured by Kyocera corporation, is chosen in this paper. The insert material is aluminum oxide and titanium carbide (Al_2O_3+TiC) and it is mainly used in semi-roughing to finishing cast iron and hardened materials. Other features of this cutting insert are listed in Table 1.

2.2 Methodology

The graphical illustration of the working principle of the MABP method is shown in Figure 1. In this system, two pairs of permanent magnets are mounted on the rotary table which is driven by a servo motor. During the polishing, the magnetic abrasives inside the chamber

Table 1 Features of the ceramic cutting insert

Symbol	Color	Component	Hardness (GPa)	Fracture toughness (MPa·m$^{1/2}$)	Transverse strength (MPa)
A65	Black	Al_2O_3+TiC	20.6	4.5	780

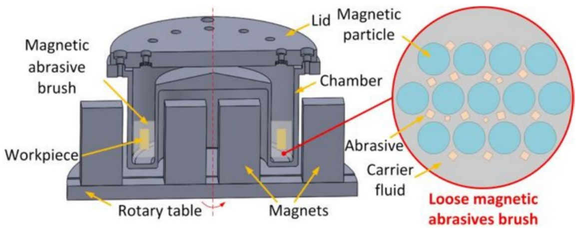

Figure 1 Graphical illustration of the working principle of the MABP system

generate the continuous rotating magnetic abrasive brush under the effect of a rotating magnetic field while the chamber is fixed on the metal frame and does not rotate. As for the magnetic abrasive brush, it is a type of loose magnetic abrasives brush which are the magnetic particles mixing with the polishing abrasives in the carrier fluid [45]. The workpiece held by the fixture is fixed in the annular chamber. Moreover, the polishing abrasives inside the continuously rotating magnetic abrasive brushes impinge the workpiece and remove material from the surface.

3 Experiments

3.1 MABP Experiments

Schematic diagram of the MABP and corresponding experimental set-up is presented in Figure 2. The apparatus was mainly composed of a lid, chamber, magnets, and rotary table. As shown in Figure 2(d), the ceramic inserts were fixed by the fixtures which were secured to the lid with a stainless screw. Two pairs of magnets were installed on the rotary table which was driven by the motor. The chamber was mounted above the magnets and did not move during the polishing. Under the magnetic field, two pairs of magnetic abrasive brushes were formed inside the chamber as shown in Figure 2(e). Moreover, these magnetic abrasive brushes which were a loose type of magnetic abrasive included carbonyl iron powder (CIP) (average size is 3 μm, BASF Co. Ltd., Germany) and diamond polishing slurry (average size is 125 nm, Universal Photonics Inc., USA) as shown in Figure 2(f). In addition, the concentration of the diamond polishing slurry was 25%. To verify the repeatability of the experiments, two inserts were polished simultaneously in this experiment. Based on

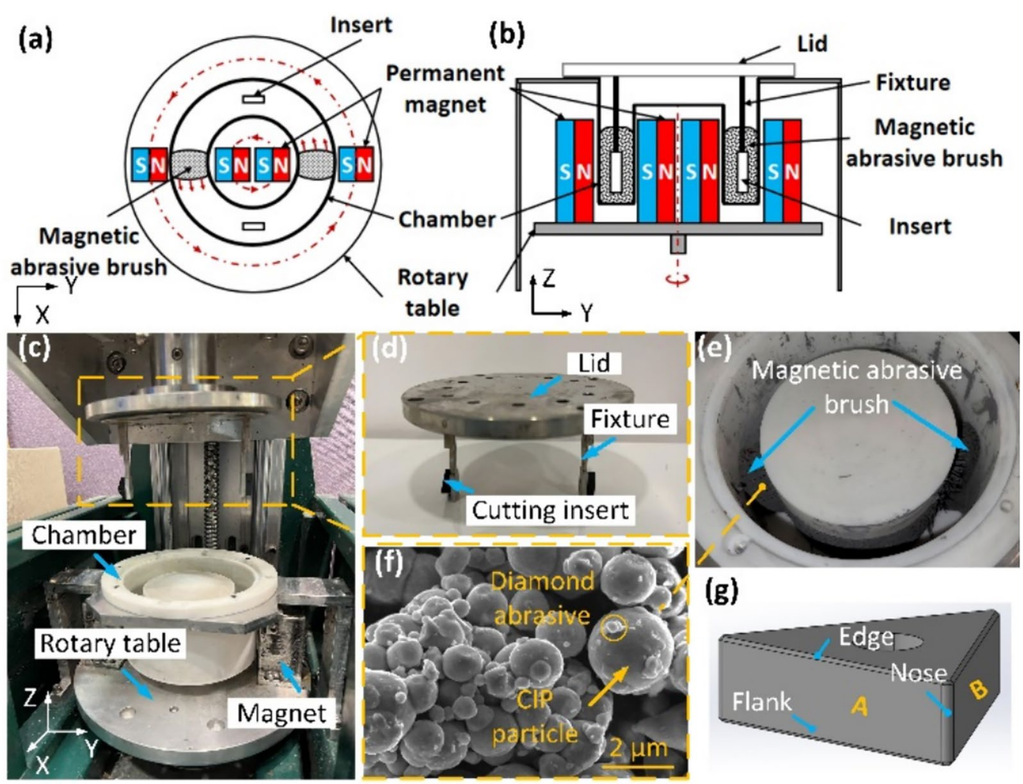

Figure 2 Schematic diagram of the MABP and corresponding experimental set-up: (**a**) Top view and (**b**) side view of the schematic diagram, (**c**) A photograph of the prototype of the MABP system, (**d**) Magnified view of the lid, (**e**) A photograph of the chamber with two magnetic brushes inside, (**f**) SEM image of the magnetic abrasive brush, (**g**) Polished and measurement positions

Table 2 MABP experimental conditions

Parameters (unit)	Values
Polishing time (min)	15
Rotational speed (r/min)	1500
Weight of magnetic abrasive (g)	60
Weight of CIP (g)	45
Weight of diamond polishing slurry (g)	15
Concentration of the polishing slurry (wt.%)	25

our previous investigation [46–48], other experimental conditions are listed in Table 2.

After polishing experiments, the samples were cleaned with an ultrasonic cleaning machine for 5 min. The measurement positions of the cutting inserts involved the edge, flank, and nose, and each side of the insert was designated by letters A and B respectively, as shown in Figure 2(g). 3D topography images and surface roughness were measured by the Zygo Nexview white light interferometer, and the magnification of the objective lens was 40. The surface roughness of each position was measured at four different points. The micro-topography of the cutting inserts was observed by a Tescan MAIA3 field emission scanning electron microscope (SEM). The element compositions of the cutting insert were analyzed by energy disperses spectroscopy (EDX). In addition, a 3D optical measuring system (Alicona IFM G4) was employed for measuring nose radius.

3.2 Cutting Experiments

To evaluate the effect of MABP polishing on cutting inserts, cutting experiments were performed on a 25 mm diameter S136H steel with hardness of 48 HRC using unpolished and polished inserts as shown in Figure 3. The cut length per pass was 80 mm in the feed direction. Other cutting experiment conditions are summarized in Table 3.

After cutting experiments, the images of flank wear were captured by the Keyence VH-6000 digital microscope, and the maximum flank wear was used to evaluate the tool life. For the experiments, the cutting operation was terminated once the insert was broken.

4 Results and Discussion

4.1 Polishing Performance of MABP on Cutting Insert

The photograph of the ceramic cutting inserts before and after polishing are presented in Figure 4, which are polished for 15 min. For both samples, the cutting insert surface successfully achieved a mirror effect after polishing as shown in Figure 4(b). It demonstrates that

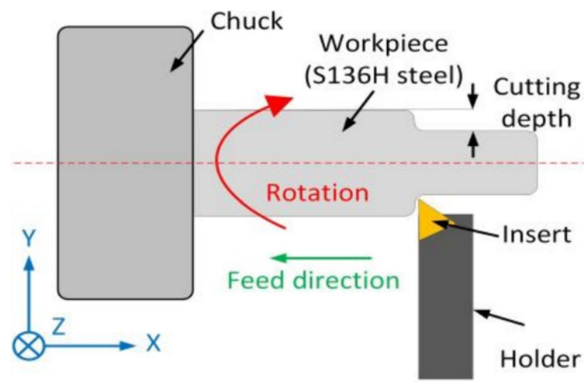

Figure 3 Schematic of the cutting experiment

Table 3 Cutting experimental conditions

Parameters (unit)	Values
Workpiece	S136H steel 48 HRC
Spindle speed (r/min)	560
Cutting depth (mm)	0.5
Feed rate (mm/r)	0.04

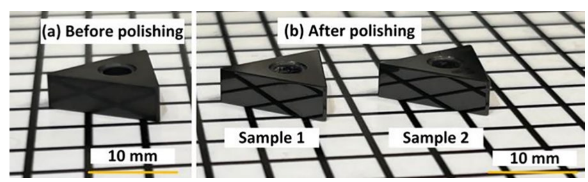

Figure 4 Photograph of the ceramic cutting inserts (**a**) before and (**b**) after polishing

MABP can achieve precision polishing of ceramic cutting inserts.

Furthermore, the 3D topography images of the cutting insert (sample 1) at flank-A, nose and edge-A are demonstrated in Figure 5. As for the flank, there are lots of machining marks because of finishing by grinding as shown in Figure 5(a). After polishing, the machining marks have been eliminated effectively, and smooth and flat surfaces are achieved, as seen in Figure 5(b). In addition, the surface roughness in regard to mean height (Sa) and maximum height (Sz) decreased rapidly from 61 nm and 687 nm to 2 nm and 29 nm, respectively. The same phenomenon can also be observed in the edge as shown in Figure 5(d)−(f). From initial 94 nm and 1031 nm, the surface roughness and maximum height of the edge dramatically decreased to 4 nm and 90 nm, respectively. In the nose case, the surface roughness showed a moderate reduction after 15 min polishing, while the maximum height went

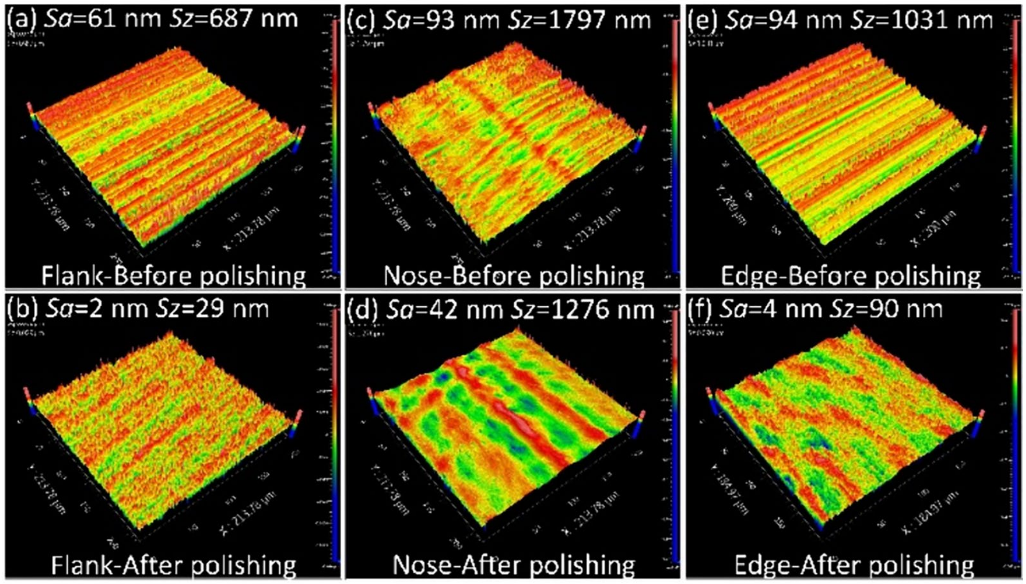

Figure 5 3D topography images of cutting insert (sample 1) at (**a**), (**b**) flank-A, (**c**), (**d**) nose and (**e**), (**f**) edge-A before and after MABP

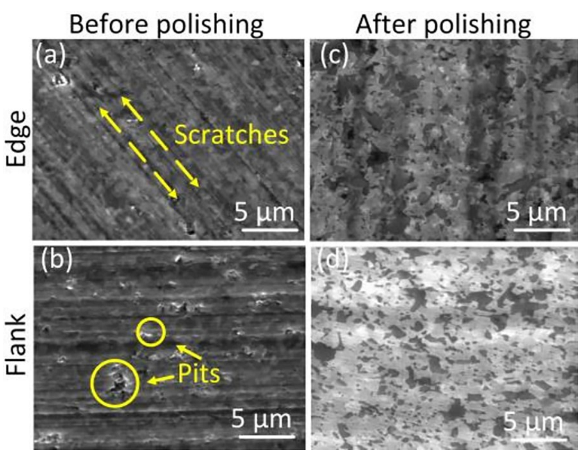

Figure 6 SEM micro-images of cutting insert (sample 2) at edge and flank (**a**), (**b**) before and (**c**), (**d**) after MABP

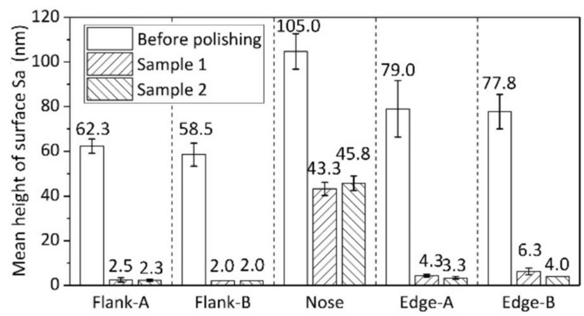

Figure 7 Average surface roughness of sample 1 and sample 2 before and after 15 min MABP

down slightly. The reason is that the impinging angle of the brush is 90°, and the magnetic abrasive particles impact the nose vertically, leading to a decrease in material removal rates [49]. On the other hand, when the brush impinges on the flank and edge, the angle is less than 90°, resulting in an increase in material removal rates due to the shear force applied.

As shown in Figure 6, the SEM micro-surface topography of the cutting insert (sample 2) at flank-B and edge-B is measured by the Tescan MAIA3 SEM. In terms of the initial surface, numerous clear scratches and pits were observed on the flank and nose after machining as shown in Figure 6(a), (b), formed during the shaping of the cutting insert by the diamond grinding wheel. After 15 min MABP, it is obviously seen in Figure 6(c), (d) that a smooth surface without any micro-defects could be achieved.

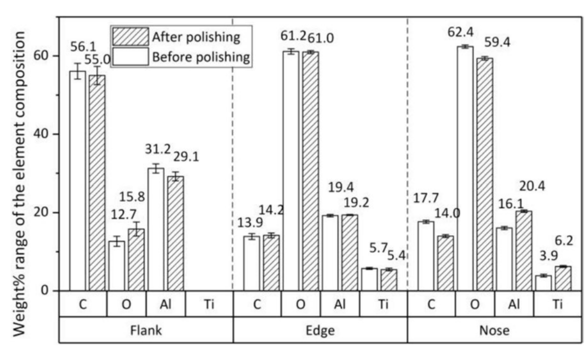

Figure 8 EDX element composition of cutting insert before and after MABP

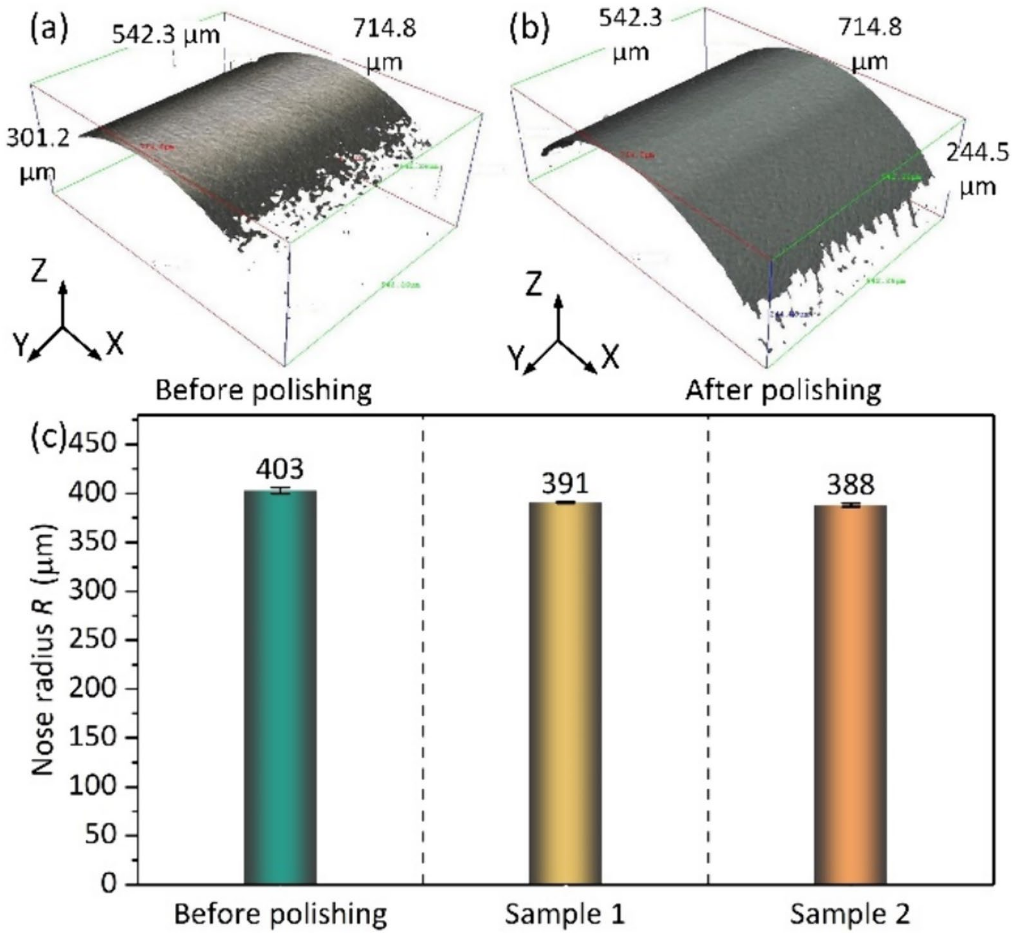

Figure 9 3D nose profile (**a**) before and (**b**) after MABP, (**c**) Average nose radius of cutting insert comparison between before and after MABP

4.2 Surface Roughness

Figure 7 comparatively describes the average Sa of the flank, nose and edge before and after 15 min polishing. Overall, the surface roughness of two cutting inserts was sharply reduced in all cases as compared with the as-received conditions. To be more specific, from initial 62.3±3.2 nm and 79±12.7 nm, the Sa of flank-A and edge-A for sample 1 steeply dropped to 2.5±1.0 nm and 4.3±0.7 nm, respectively. The same trend could also be observed in flank-B and edge-B of sample 1. However, the effect of MABP on the surface roughness of the nose was not as obvious as that on the flank and edge. These results are likely to be related to the nose with a complex shape and much higher initial surface roughness. In addition, sample 2 and sample 1 were more equally represented in the value of average surface roughness of the flank, nose and edge. It indicates that MABP exhibits great potential for batch polishing, which can achieve the polishing of multiple cutting inserts to improve processing efficiency.

4.3 Element Composition

EDX tests were conducted to analyze any differences in the material before and after the polishing process. Figure 8 provides the experimental data on the wt.% range of the element composition before and after MABP. The EDX results showed that the cutting insert (including flank, edge, and nose) consisted of C, O, Al, and Ti. After polishing, insert surfaces showed an elemental composition of C, O, Al, and Ti as well. To be more specific, the wt.% of Al increased slightly after MABP, increasing by about 2.0%, 0.2%, and 4.3% corresponding to flank, edge, and nose, respectively. In the contrast, the wt.% of O declined around 3.1%, 0.2%, and 3.0% corresponding to flank, edge, and nose, respectively. As for other elements, a moderate fluctuation could be observed in wt.%. In summary, the element composition does not significantly change in ceramics cutting insert after MABP. This indicates that there is no grain refinement due to mechanical load

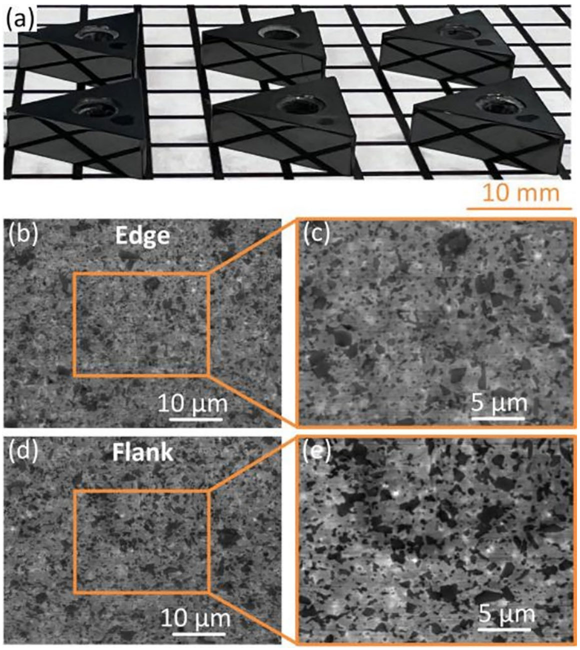

Figure 10 Batch polishing performance: (**a**) Photograph of the ceramic cutting inserts after batch polishing, SEM micro-images of cutting insert (**b**), (**c**) edge and (**d**), (**e**) flank after batch polishing

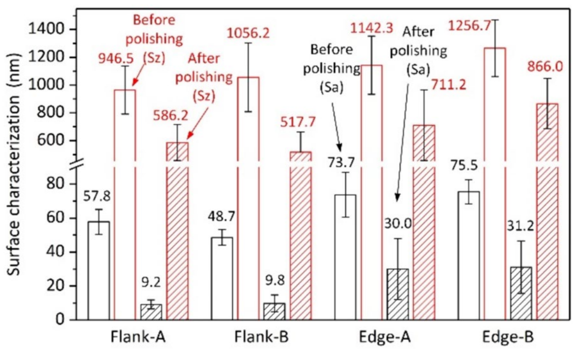

Figure 11 Height roughness parameters of flank and edge before and after batch polishing

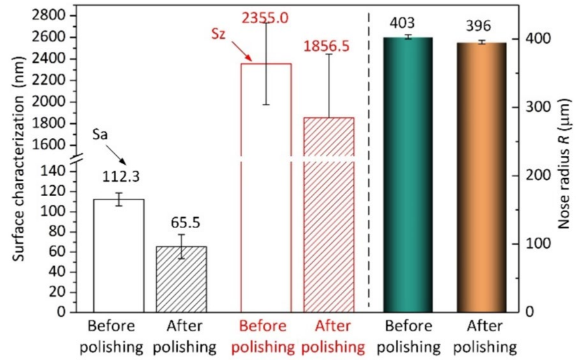

Figure 12 Height roughness parameters and radius of inserts nose before and after batch polishing

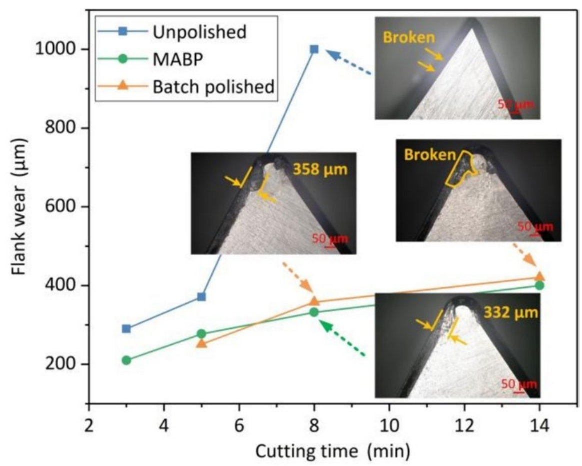

Figure 13 Changes in the maximum flank wear with cutting time

or chemical changes resulting from high temperatures during the polishing procedure.

4.4 Nose Radius

Figure 9(a) and (b) present the 3D nose profile before and after MABP, respectively. It should be noted that the nose is rounded after polishing. Moreover, Figure 9(c) gives information about the average nose radius before and after polishing. For the as-received insert, the average nose radius was 403 μm. After 15 min MABP, the average nose radii of sample 1 and sample 2 were 391 μm and 388 μm, respectively, and both of these two samples were characterized by small standard deviations (SD). It indicates that a sharp nose can be obtained, and the nose radius only decreases narrowly after MABP.

4.5 Application of MABP for Multiple Cutting Inserts

If a batch system is realized in MABP, the time needed for MABP of inserts can be further reduced. A total of six inserts were fixed on the lid through fixtures for simultaneous batch polishing. The photograph of the ceramic cutting inserts after batch polishing is shown in Figure 10(a). In terms of all the inserts, the mirror effect could be successfully obtained after 15 min polishing. It indicates that MABP can achieve the precision polishing of a batch of ceramic cutting inserts simultaneously in a short time. Furthermore, the SEM micro-images of the inserts edge and flank measured by Tescan MAIA3 SEM are shown in Figure 10(b)–(e). After batch polishing, the machining marks (e.g., scratches and pits) on the edge and flank were efficiently removed.

In addition, the height roughness parameters of the flank and edge after batch polishing is presented in Figure 11. In general, the average Sa were all improved after batch polishing. From initial 57.8±7.3 nm and 73.7±13.1 nm, the average surface roughness at flank-A and edge-A deceased sharply to 9.1±2.6 nm and 30.0±17.9 nm, respectively. Meanwhile, the same trend could also be observed for flank-B and edge-B. As for the surface roughness in terms of the Sz, it was also reduced moderately from 946.5±173.9 nm to 586.2±129.2 nm at flank-A and from 1142.3±210.3 nm to 711.2±254.3 nm at edge-A, respectively.

Figure 12 shows the experimental data on nose height roughness parameters and radius before and after batch polishing. From the figure, it could be seen that the height roughness parameters of decreases gradually from Sa 112.3±6.5 nm to Sa 65.5±11.9 nm and Sz 2355.0±379.8 nm to Sz 1856.5±587.8 nm after batch polishing, respectively. In the contrast, a slight decrease in nose radius could be observed after batch polishing. Taken together, the MABP method enables batch polishing, which can allow the polishing of multiple ceramic cutting inserts to improve the polishing efficiency and accuracy in a short time. However, compared with two cutting inserts, surface roughness increases gradually for the polishing batch of inserts. It appears possible that these findings are attributed to the decreased mobility of the polishing slurry, as the velocity differential between the inserts and the polishing fluid diminishes, leading to a reduction in shear force [50].

5 Cutting Performance and Insert Wear

Figure 13 presents the changes in the maximum flank wear of polished and unpolished inserts with cutting time. At the early cutting stage, there was no clear difference in the maximum flank among MABP inserts and batch-polished inserts. The value of unpolished inserts was slightly larger than theirs. Subsequently, the maximum flank wear of unpolished inserts increased rapidly, while a moderate growth could be observed in the maximum flank wear of polished inserts. It should be noted that the unpolished insert was broken after cutting for 8 min, and the maximum flank wear of the MABP insert and batch polished insert was 332 μm and 358 μm, respectively as shown in Figure 13. With the increasing cutting time, the batch polished insert was also broken, and the batch polished inserts have the tool life of up to 1.75 times as long as unpolished inserts. These relationships can be explained by the insert surface condition. The polished inserts with a smooth surface can reduce the friction on the chip-insert interface, and result in extended tool life.

6 Conclusions

This paper presents a novel magnetic field-assisted batch polishing (MABP) method for polishing ceramics cutting inserts and evaluates tool life after polishing by MABP. The specific conclusions of this study can be summarized as follows:

(1) The MABP method enables batch polishing, which can allow the polishing of multiple ceramic cutting inserts to improve the polishing efficiency and accuracy in a short time.
(2) The surface roughness in regard to Sa less than 2.5 nm on the flank and less than 6.25 nm on the edge and less than 45.8 nm on the nose could be achieved after 15 min of MABP.
(3) The nose radii of inserts decrease slightly after MABP, indicating that MABP has a superior performance on form maintainability during polishing.
(4) The MABP-processed inserts can extend the tool life. In the S136H steel cutting, batch-polished inserts have a tool life of up to 1.75 times as long as unpolished inserts.

Acknowledgements
Not applicable.

Authors' Contributions
RG wrote the manuscript and carried out experiments; CW was in charge of the whole research and modified the manuscript; YL assisted with the experiments; XL and CC modified the manuscript. All authors read and approved the final manuscript.

Funding
Supported by Research Grants Council of the Government of the Hong Kong Special Administrative Region of China (Grant No. 15203620), Research and Innovation Office of The Hong Kong Polytechnic University of China (Grant Nos. BBXN, 1-W308), Research Studentships (Grant No. RH3Y), State Key Laboratory of Mechanical System and Vibration of China (Grant No. MSV202315).

Declarations

Competing Interests
The authors declare no competing financial interests.

Received: 1 July 2023 Revised: 25 June 2024 Accepted: 5 July 2024
Published online: 01 August 2024

References

[1] S H An, R Foest, K Fricke, et al. Pretreatment of cutting tools by plasma electrolytic polishing (PEP) for enhanced adhesion of hard coatings. *Surface and Coatings Technology*, 2021, 403: 126504.
[2] W Fan, W Ji, L H Wang, et al. A review on cutting tool technology in machining of Ni-based superalloys. *International Journal of Advanced Manufacturing Technology*, 2020, 110(11-12): 2863-2879.

[3] J Guo, X Y Wang, Y Zhao, et al. On-machine measurement of tool nose radius and wear during precision/ultra-precision machining. *Advances in Manufacturing*, 2022, 10(3): 368-381.
[4] P Olander, J Heinrichs. On wear of WC-Co cutting inserts in turning of Ti6Al4V-a study of wear surfaces. *Tribology-Materials Surfaces & Interfaces*, 2021, 15(3): 181-192.
[5] Y Touggui, S Belhadi, A Uysal, et al. A comparative study on performance of cermet and coated carbide inserts in straight turning AISI 316L austenitic stainless steel. *International Journal of Advanced Manufacturing Technology*, 2021, 112(1-2): 241-260.
[6] D B Hong, Z B Yin, F Z Guo, et al. Improvement of cutting performance of high x value α/β-SiAlON ceramic cutting inserts via tailoring microstructure and oxidation behavior. *International Journal of Refractory Metals & Hard Materials*, 2023, 111: 106087.
[7] C M Rao, B Sachin, S S Rao, et al. Minimum quantity lubrication through the micro-hole textured PCD and PCBN inserts in the machining of the Ti-6Al-4V alloy. *Tribology International*, 2020, 153: 106619.
[8] M Kuruc, T Vopat, J Moravcikova, et al. The precision analysis of cutting edge preparation on CBN cutting inserts using rotary ultrasonic machining. *Micromachines*, 2022, 13(10): 1562.
[9] S Khatai, A K Sahoo, R Kumar, et al. On Machining behaviour of various cutting Inserts: A review on hardened steel. *Materials Today-Proceedings*, 2022, 62: 3485-3492.
[10] P K Prajapati, P Biswas, B K Singh, et al. Reinforcing potential of MWCNTs on mechanical and machining performance of hot-pressed ZTA-MgO ceramic cutting inserts. *Diamond & Related Materials*, 2023, 138: 110202.
[11] B K Singh, S Goswami, K Ghosh, et al. Performance evaluation of self lubricating CuO added ZTA ceramic inserts in dry turning application. *International Journal of Refractory Metals & Hard Materials*, 2021, 98: 105551.
[12] X L Liang, Z Q Liu, B Wang, et al. Friction behaviors in the metal cutting process: state of the art and future perspectives. *International Journal of Extreme Manufacturing*, 2022, 5(1): 12002.
[13] B H Lyu, M F Ke, L Fu, et al. Experimental study on the brush tool-assisted shear-thickening polishing of cemented carbide insert. *International Journal of Advanced Manufacturing Technology*, 2021, 115(7-8): 2491-2504.
[14] M J Bermingham, J Kirsch, S Sun, et al. New observations on tool life, cutting forces and chip morphology in cryogenic machining Ti-6Al-4V. *International Journal of Machine Tools and Manufacture*, 2021, 51(6): 500-511.
[15] X Song, H Wang, X C Wang, et al. Fabrication and evaluation of diamond thick film-Si3N4 brazed cutting tool by microwave plasma chemical vapor deposition method. *Journal of Materials Processing Technology*, 2021, 291: 117034.
[16] S Mikhailov, N Kovelenov. Improving useful life of assembled cutting tools by designing a modified flank geometry in indexable cutting inserts. *Journal of Physics: Conference Series*, 2021, 1753(1): 12067.
[17] Y C Lin, S J He, D B Lai, et al. Wear mechanism and tool life prediction of high-strength vermicular graphite cast iron tools for high-efficiency cutting. *Wear*, 2020, 454: 203319.
[18] S Chaabani, P J Arrazola, Y Ayed, et al. Comparison between cryogenic coolants effect on tool wear and surface integrity in finishing turning of Inconel 718. *Journal of Materials Processing Technology*, 2020, 285: 116780.
[19] R S Revuru, J Z Zhang, N R Posinasetti. Comparative performance studies of turning 4140 steel with TiC/TiCN/TiN-coated carbide inserts using MQL, flooding with vegetable cutting fluids, and dry machining. *International Journal of Advanced Manufacturing Technology*, 2020, 108(1-2): 381-391.
[20] B D Jerold, M P Kumar. The Influence of cryogenic coolants in machining of Ti-6Al-4V. *Journal of Manufacturing Science and Engineering-Transactions of the ASME*, 2013, 135(3): 031005.
[21] A Iturbe, E Hormaetxe, A Garay, et al. Surface integrity analysis when machining Inconel 718 with conventional and cryogenic cooling. *Procedia CIRP*, 2016, 45: 67-70.
[22] X Tong, P Han, S C Yang. Coating and micro-texture techniques for cutting tools. *Journal of Materials Science*, 2022, 57(36): 17052-17104.
[23] S Dabees, S Mirzaei, P Kaspar, et al. Characterization and evaluation of engineered coating techniques for different cutting tools-review. *Materials*, 2022, 15(16): 5633.
[24] X C Wang, C C Wang, C Y Wang, et al. Approach for polishing diamond coated complicated cutting tool: Abrasive flow machining (AFM). *Chinese Journal of Mechanical Engineering*, 2018, 31(1): 97.
[25] S W Tang, P F Liu, Z Su, et al. Preparation and cutting performance of nanoscaled Al2O3-coated micro-textured cutting tool prepared by atomic layer deposition. *High Temperature Materials and Processes*, 2021, 40: 77-86.
[26] L Yin, A C Spowage, K Ramesh, et al. Influence of microstructure on ultraprecision grinding of cemented carbides. *International Journal of Machine Tools and Manufacture*, 2004, 44(5): 533-543.
[27] H Yamaguchi, P Hendershot, R Pavel, et al. Polishing of uncoated cutting tool surfaces for extended tool life in turning of Ti-6Al-4V. *Journal of Manufacturing Processes*, 2016, 24: 355-360.
[28] Z H Hu, C J Qin, X G Chen, et al. Chemical-mechanical polishing of cemented carbide insert surface for extended tool life in turning of GH4169 nickel-based superalloy. *International Journal of Precision Engineering and Manufacturing*, 2020, 21(8): 1421-1435.
[29] M Yoshikawa, F Okuzumi. Hot-iron-metal polishing machine for CVD diamond films and characteristics of the polished surfaces. *Surface and Coatings Technology*, 1997, 88(1-3): 197-203.
[30] B H Lyu, Q K He, S H Chen, et al. Experimental study on shear thickening polishing of cemented carbide insert with complex shape. *International Journal of Advanced Manufacturing Technology*, 2019, 103(1-4): 585-595.
[31] H Yamaguchi, A K Srivastava, M Tan, et al. Magnetic abrasive finishing of cutting tools for high-speed machining of titanium alloys. *CIRP Journal of Manufacturing Science and Technology*, 2014, 7(4): 299-304
[32] Y Tanaka, H Sato, O Eryu. Improved cemented carbide tool edge formed by solid phase chemical-mechanical polishing. *Journal of Materials Research and Technology*, 2022, 20: 606-615.
[33] H Tanaka, Y Kawase, Y Akagami. Novel polishing method of cutting edge using AC electric field for controlling flank wear. *Key Engineering Materials*, 2018, 767: 268-274.
[34] D Ishimaru, M Touge, H Muta, et al. Burr suppression using sharpened PCD cutting edge by ultraviolet-ray irradiation assisted polishing. *Procedia CIRP*, 2012, 1: 184-189.
[35] Y Izumi, K Goto, T Sakamoto, et al. Advancement of PCD cutting tools by UV-polishing and their cutting performance. *Journal of the Japan Society for Abrasive Technology*, 2017, 61(4): 210-215.
[36] E Uhlmann, H Riemer, S An, et al. Ecological and functional optimizationof the pretreatment process for plasma based coatings of cutting tools. *Procedia Manufacturing*, 2019, 33: 618-624.
[37] C J Wang, Z Z Wang, Q J Wang, et al. Improved semirigid bonnet tool for high-efficiency polishing on large aspheric optics. *International Journal of Advanced Manufacturing Technology*, 2017, 88(5-8): 1607-1617.
[38] X P Huang, Z Z Wang, Z W Lin. Movement modeling and control for robotic bonnet polishing. *Chinese Journal of Mechanical Engineering*, 2022, 35: 68.
[39] M Schneckenburger, R Almeida, S Höfler, et al. Material removal by slurry erosion in the robot polishing of optics by polishing slurry nozzles. *Wear*, 2022, 494-495: 204257.
[40] C J Wang, C F Cheung, L T Ho, et al. A novel multi-jet polishing process and tool for high-efficiency polishing. *International Journal of Machine Tools and Manufacture*, 2017, 115: 60-73.
[41] C Jiang, J L Huang, Z Y Jiang, et al. Estimation of energy savings when adopting ultrasonic vibration-assisted magnetic compound fluid polishing. *International Journal of Precision Engineering and Manufacturing-Green Technology*, 2019, 8(1): 1-11.
[42] C Jiang, R Gao, Y Hao, et al. Investigation of indentation zone on K9 glass under ultrasonic vibration condition using an equivalent mean contact pressure. *Experimental Techniques*, 2019, 43(6): 657-666.
[43] D W Tan, Z W Chen, W X Wei, et al. Wear behavior and mechanism of TiB2-based ceramic inserts in high-speed cutting of Ti6Al4V alloy. *Ceramics International*, 2020, 46(6): 8135-8144.
[44] M E R Bonifacio, A E Diniz. Correlating tool wear, tool life, surface roughness and tool vibration in finish turning with coated carbide tools. *Wear*, 1994, 173(1-2): 137-144.
[45] C J Wang, C F Cheung, L T Ho, et al. A novel magnetic field-assisted mass polishing of freeform surfaces. *Journal of Materials Processing Technology*, 2020, 279: 116552.

[46] C J Wang, Y M Loh, C F Cheung, et al. Shape-adaptive magnetic field-assisted batch polishing of three-dimensional surfaces. *Precision Engineering*, 2020, 76: 261-283.
[47] C J Wang, Y M Loh, C F Cheung, et al. Magnetic field-assisted batch super finishing on thin-walled components. *International Journal of Mechanical Sciences*, 2022, 223: 107279.
[48] Y M Loh, R Gao, C F Cheung, et al. A novel magnetic field assisted automatic batch polishing method for dental ceramic crowns. *Ceramics International*, 2023, 49(16): 26540-26547.
[49] H Huang, X L Li, D K Mu, et al. Science and art of ductile grinding of brittle solids. *International Journal of Machine Tools and Manufacture*, 2021, 161: 103675.
[50] B R Lawn, H Huang, M Y Lu, et al. Threshold damage mechanisms in brittle solids and their impact on advanced technologies. *Acta Materialia*, 2022, 232: 117921.

Rui Gao born in 1994, is currently a postdoctoral fellow at *State Key Laboratory of Ultra-precision Machining Technology, Department of Industrial and Systems Engineering, The Hong Kong Polytechnic University, China*. He received his Ph.D. degree from *University of Shanghai for Science and Technology, China*, in 2023. His research interests include advanced manufacturing technology and semiconductor processing.

Chunjin Wang born in 1988, is currently an assistant professor at *The Hong Kong Polytechnic University, China*. He received his Ph.D. degree from *Xiamen University, China*, in 2015. His research interests include ultra-precision polishing technology, ultra-precision machining equipment and instrumentation, advanced optics manufacturing and functional surface engineering.

Loh Yee Man born in 1997, is currently a Ph.D. candidate at *The Hong Kong Polytechnic University, China*. She received her bachelor degree from *The Hong Kong Polytechnic University, China*, in 2018. Her research interests focus on ultra-precision manufacturing technology, surface finishing and magnetic field-assisted polishing technology.

Xiaoliang Liang born in 1991, is currently a postdoctoral fellow at *State Key Laboratory of Ultra-Precision Machining Technology, Department of Industrial and Systems Engineering, The Hong Kong Polytechnic University, China*. He received his Ph.D. degree from *Shandong University, China*, in 2021.

Chen Jiang born in 1978, is currently a professor at *University of Shanghai for Science and Technology, China.* He received his Ph.D. degree from *Xiamen University, China*, in 2011.

Chi Fai Cheung born in 1970, is currently the chair professor at *The Hong Kong Polytechnic University, China*. He received his Ph.D. degree from *The Hong Kong Polytechnic University, China*, in 2000. His research interests include precision engineering, knowledge and technology management, as well as enterprise systems.